

## Letter of Intent

## A universal setup for kinematical complete measurements of Reactions with Relativistic Radioactive Beams (R<sup>3</sup>B)

### The R<sup>3</sup>B collaboration

14 April 2004

#### Abstract

A versatile reaction setup with unprecedented efficiency, acceptance, and resolution for kinematically complete measurements of reactions with high-energy radioactive beams is proposed. The setup will be located at the focal plane of the high-energy branch of the Super-FRS. The experimental configuration is based on a concept similar to the existing LAND reaction setup at GSI introducing substantial improvement with respect to resolution and an extended detection scheme, which comprises the additional detection of light (target-like) recoil particles and a high-resolution fragment spectrometer. The setup is adapted to the highest beam energies (corresponding to 20 Tm magnetic rigidity) provided by the Super-FRS capitalizing on the highest possible transmission of secondary beams. The experimental setup is suitable for a wide variety of scattering experiments, i.e., such as heavy-ion induced electromagnetic excitation, knockout and breakup reactions, or light-ion (in)elastic and quasi-free scattering in inverse kinematics, thus enabling a broad physics programme with rare-isotope beams to be performed.

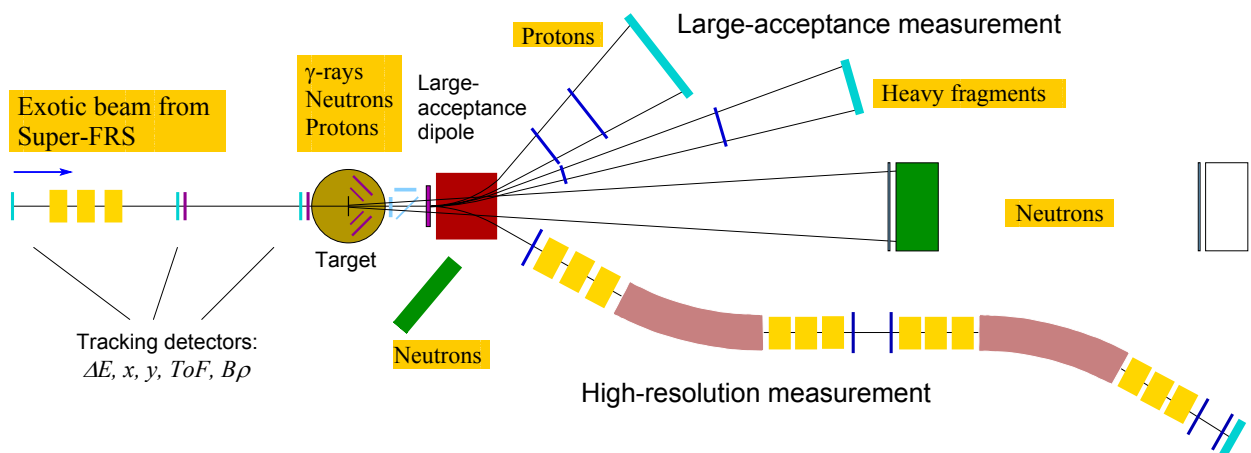


*Figure 1: Schematic drawing of the experimental setup comprising  $\gamma$ -ray and target recoil detection, a large-acceptance dipole magnet, a high-resolution magnetic spectrometer, neutron and light-charged particle detectors, and a variety of heavy-ion detectors.*

## **The R<sup>3</sup>B Collaboration**

Aarhus, Denmark, University of Aarhus

D.V. Fedorov, H.O.U. Fynbo, A.S. Jensen, K.-H. Langanke, K. Riisager

Argonne, USA, Argonne National Laboratory

J. Nolen

Bergen, Norway, University of Bergen

J.S. Vaagen

Birmingham, UK, University of Birmingham

M. Freer

Caen, France, GANIL

D. Boilley, C.E. Demonchy, W. Mittag, P. Roussel-Chomaz, H. Savajols

Daresbury, UK, CCLRC Daresbury Laboratory

R. Lemmon, J. Simpson, D. Warner

Darmstadt, Germany, Technische Universität

J. Enders, T. Nilsson, A. Richter, G. Schrieder

Darmstadt, Germany, GSI

T. Aumann, F. Becker, K. Boretzky, P. Egelhof, H. Emling, H. Feldmeier, H. Geissel, J. Gerl, M. Gorska, V. Henzl, J. Hoffmann, D. Henzlova, A. Kelic, I. Kojouharov, N. Kurz, G. Münzenberg, T. Neff, M.V. Ricciardi, T. Saito, K.-H. Schmidt, H. Simon, K. Sümmerer, W. Trautmann, S. Typel, H. Weick, O.Yordanov

Debrecen, Hungary, ATOMKI

A. Algora, M. Csatlós, Z. Gácsi, J. Gulyás, M. Hunyadi, A. Krasznahorkay

Dresden, Germany, Forschungszentrum Rossendorf

E. Grosse, A. Wagner

Dubna, Russia, Joint Institute for Nuclear Research

S.N. Ershov, L. Grigorenko

East Lansing, USA, NSCL, MSU

B. Sherrill

Gatchina, Russia, Petersburg Nuclear Physics Institute, PNPI

A. Khanzadeev

Giessen, Germany, Justus-Liebig-Universität

H. Lenske, M. Winkler

Gif sur Yvette, France, DAPNIA, CEA Saclay

N. Alamanos, A. Boudard, J.-E. Ducret, B. Gastineau, E. Le Gentil, V. Lapoux, S. Leray, S. Pietri, E. Pollacco, C. Volant

Göteborg, Sweden, Chalmers University of Technology

H. Johansson, B. Jonson, M. Meister, G. Nyman, M. Zhukov

Guildford, UK, University of Surrey

J. Al Khalili, W. Catford, W. Gelletly, R. Johnson, M. Oi, Z. Podolyak, P. Regan, P. Stevenson, I. Thompson, J. Tostevin, P. Walker

Heidelberg, Germany, Max-Planck-Institut

Heiko Scheit

Keele, UK, University of Keele

M. Bentley

Köln, Germany, Universität zu Köln

P. Reiter

Kolkata, Saha Institute of Nuclear Physics, India  
U. Datta Pramanik

Krakow, Poland, Jagellonski University  
P. Adrich, M. Kajetanowicz, A. Klimkiewicz, K. Korcyl, R. Kulesza

Krakow, IFJ PAN Krakow  
A. Maj

Liverpool, UK, University of Liverpool  
M. Chartier, P. Nolan

Lyon, IPN Lyon, France  
Ch. Schmitt

Madrid, Spain, Instituto de Estructura de la Materia, CSIC  
M.J.G. Borge, L.M. Fraile, E. Garrido, O. Tengblad

Mainz, Germany, Johannes Gutenberg Universität  
O. Kiselev, J.V. Kratz

Manchester, UK, University of Manchester  
D. Cullen, S. Freeman

Moscow, Russia, Kurchatov Institute  
L. Chulkov, B. Danilin

Moscow, Russia, Institute for Nuclear Research, Russian Academy of Sciences  
A. Botvina

Mumbai, India, Tata Institute of Fundamental Research  
R. Palit

München, Germany, TU München  
M. Böhmer, T. Faestermann, J. Friese, R. Gernhäuser, T. Kröll, R. Krücken

Obninsk, Russia, IPPE Obninsk  
A. Ignatyuk

Orsay, France, IN2P3/IPN Orsay  
Ch.-O. Bacri, Y. Blumenfeld, E. Khan, F. Rejmund, J.A. Scarpaci

Paisley, UK, University of Paisly  
R. Chapman, M. Labiche, X. Liang, K. Spohr

Pyhäsalmi, Finland, CUPP project  
T. Enqvist

RIKEN, Japan  
R. Kanungo

Santiago de Compostela, Spain, Univers. of SdC  
J. Benlliure, D. Cortina-Gil, I. Duran

Valencia, Spain, CSIC-University  
B. Rubio, J.L. Tain

Yale University, USA  
A. Heinz

York, UK, University of York  
Ch. Barton

Spokesperson: T. Aumann E-Mail: t.aumann@gsi.de

Deputy: B. Jonson E-Mail: bjn@fy.chalmers.se

## **Contents**

1. Introduction and overview
  - 1.1. Experimental concept
  - 1.2. Physics and reactions to be studied with R<sup>3</sup>B
    - 1.2.1 Total-absorption measurements
    - 1.2.2 Elastic proton scattering
    - 1.2.3 Knockout reactions
    - 1.2.4 Quasi-free scattering
    - 1.2.5 Electromagnetic excitation
    - 1.2.6 Charge-exchange reactions
    - 1.2.7 Fission
    - 1.2.8 Spallation reactions
    - 1.2.9 Projectile fragmentation and multifragmentation
    - 1.2.10 Astrophysics
2. Detector subsystems
  - 2.1 Superconducting large-acceptance dipole
  - 2.2 High-resolution spectrometer
  - 2.3 Tracking detectors and velocity measurements
  - 2.4 Gamma detection
  - 2.5 Proton recoil detector
  - 2.6 Low-energy neutron detector
  - 2.7 High-resolution neutron time-of-flight spectrometer
  - 2.8 Multi-track ion detector for spallation and fission measurements
3. Trigger and data acquisition system
4. Physics performance
5. Implementation
  - 5.1 Experimental area and radiation environment
  - 5.2 Cost estimates
  - 5.3 Organisation and responsibilities
  - 5.4 Time schedule
  - 5.5 Beam time considerations

## References

## 1. Introduction and overview

### 1.1. Experimental concept

During the past decade it has been demonstrated that reactions with high-energy secondary beams are an important tool to explore properties of nuclei far off stability, which allows detailed spectroscopic information to be extracted. The physics motivation for studying reactions with exotic nuclei is described extensively in various reports in the context of next-generation facilities, see, e.g., the 'Conceptual Design Report' (CDR) (<http://www.gsi.de/GSI-Future/cdr>) for the future FAIR project. High beam energies, in the range of a few hundred MeV/nucleon, allow a quantitative description of the reaction mechanisms [AIK03], while also having experimental merits, such as the possibility of using relatively thick targets (in the order of 1 g/cm<sup>2</sup>). Moreover, due to the kinematical forward focusing full-acceptance measurements are feasible with moderately sized detectors. This makes it possible to gain nuclear-structure information from reaction studies even with very low beam intensities, as low as about 1 ion/s.

R<sup>3</sup>B will cover experimental reaction studies with exotic nuclei far off stability, with emphasis on nuclear structure and dynamics. Astrophysical aspects and technical applications are also concerned. A survey of reaction types and associated physics goals that can be achieved is given in Table 1. A brief description follows subsequently in the next sub-section, for a more detailed discussion we refer to the CDR. In case of light-ion scattering, the experiments at R<sup>3</sup>B are complementary to the ones proposed for the internal target in the NESR (see the LoI of the EXL collaboration). Here, the R<sup>3</sup>B programme will focus on the most exotic short-lived nuclei, which cannot be stored and cooled efficiently, and on reactions with large-momentum transfer allowing the use of thick targets. The proposed experimental setup is adapted to the highest beam energies delivered by the Super-FRS, thus exploiting fully the highest possible transmission efficiency of secondary beams.

*Table 1. Reaction types with high-energy beams measurable with R<sup>3</sup>B and corresponding achievable information*

<i>Reaction type</i>	<i>Physics goals</i>
Total-absorption measurements	Nuclear matter radii, halo and skin structures
Elastic p scattering	Nuclear matter densities, halo and skin structures
Knockout	Shell structure, valence-nucleon wave function, many-particle decay channels unbound states, nuclear resonances beyond the drip lines
Quasi-free scattering	Single-particle spectral functions, shell-occupation probabilities, nucleon-nucleon correlations, cluster structures
Heavy-ion induced electromagnetic excitation	Low-lying transition strength, single-particle structure, astrophysical S factor, soft coherent modes, low-lying resonances in the continuum, giant dipole (quadrupole) strength
Charge-exchange reactions	Gamow-Teller strength, soft excitation modes, spin-dipole resonance, neutron skin thickness
Fission	Shell structure, dynamical properties
Spallation	Reaction mechanism, astrophysics, applications: nuclear-waste transmutation, neutron spallation sources
Projectile fragmentation and multifragmentation	Equation-of-state, thermal instabilities, structural phenomena in excited nuclei, $\gamma$ -spectroscopy of exotic nuclei

The proposed experimental scheme is based on that of the LAND apparatus which is used successfully in experiments with secondary beams from the FRS facility at GSI. The most essential upgrades concern the target recoil detector and the two magnetic spectrometers. A schematic view of the R<sup>3</sup>B experimental setup is shown in Figure 1. The incoming secondary beams are tracked and identified on an event-by-event basis. Measurements of the magnetic rigidity  $B\rho$  (position measurement at the dispersive focus in the Super-FRS), time-of flight ToF, and energy loss  $\Delta E$  provide unique isotope identification and momentum determination. Although the secondary beam has a momentum spread of  $\pm 2.5\%$ , the

momentum will be determined to an accuracy of  $10^{-4}$  (event-wise). After the secondary target, the kinematically forward focused projectile residues are again identified and momentum analyzed.

Two modes of operation are foreseen depending on the demands of the experiments: i) A large-acceptance mode: Heavy fragments and light charged particles (i.e. protons) are deflected by a large-acceptance dipole and detected with full solid-angle acceptance, for most reactions envisaged (left bend in Figure 1). Resolutions for velocity and  $B\rho$  measurements amount to about  $10^{-3}$  allowing unique identification in mass and nuclear charge of also heavy fragments. ii) A high-resolution mode: here, the dipole magnet is operated in reversed mode, deflecting the fragments into a magnetic spectrometer (right bend in Figure 1). The envisaged resolution of  $10^{-4}$  will allow, e.g., a precise measurement of the fragment recoil momentum in single-nucleon knockout and quasi-free scattering experiments even for heavy nuclei.

The large gap of the dipole provides a free cone of  $\pm 80$  mrad for the neutrons, which are detected in forward direction by the large area neutron detector (new LAND). At beam energies around 500 MeV/nucleon, this corresponds to a 100% acceptance for neutrons with kinetic energies up to 5 MeV in the projectile rest frame. Depending on the requirements on resolution and acceptance, the detector with an active area of  $2 \times 2$  m<sup>2</sup> is placed at a distance of 10 m to 35 m from the target.

The target is surrounded by a gamma-ray spectrometer. For most of the experiments envisaged, a high-efficiency total-absorption spectrometer (cooled CsI) is the optimum solution, which is also used to measure the energy of recoiling protons. For specific experiments requiring ultimate energy resolution for  $\gamma$ -detection, the Germanium spectrometer AGATA might be used alternatively. For elastic, inelastic and quasi-free scattering experiments or charge-exchange reactions, liquid hydrogen or frozen hydrogen targets are considered. Recoiling protons and neutrons are detected by a Si-strip array and plastic scintillators, respectively. For measurements at low momentum transfer, the use of an active target is foreseen. Fast neutrons stemming from (p,pn) type knockout processes can be measured by placing part of the LAND detector at angles around 45 degrees. The Si-strip array is also used as a high-granularity multiplicity detector array for measuring charged particles from the fire-ball, created in semi-peripheral collisions. The detector subsystems needed to achieve such a kinematical complete measurement of reactions with high efficiency and acceptance, which is of key importance for experiments with radioactive beams, are described in section 2 of this Letter of Intent.

## 1.2. Physics and reactions to be studied with R<sup>3</sup>B

### 1.2.1. Total-absorption measurements

Nuclear *matter radii* may be inferred from total interaction cross sections derived from total-absorption measurements of radioactive ions in thick targets. This technique requires intensities of the order of only one ion/s. For instance, interesting results were obtained by a RIKEN-GSI collaboration [Suz95] by using beams of unstable sodium isotopes. These data, together with isotope-shift measurements, provide a first experimental manifestation of *neutron skins*. Beam intensities available at the new facility will allow systematic studies of this phenomenon in heavy nuclei. Such experiments can be performed using the high-resolution spectrometer after the dipole magnet.

### 1.2.2. Elastic proton scattering

The radial shape of the *nuclear density distribution* of exotic nuclei may be extracted from high-energy proton elastic scattering in inverse kinematics. Previous measurements [Ege02] using secondary beams at 700 MeV/nucleon have demonstrated the power of the method to investigate *halo* and *skin* structures in nuclei far off stability. Complementary to the experiments proposed at the storage ring, elastic scattering will be measured at R<sup>3</sup>B using (thick) liquid hydrogen or frozen hydrogen targets, and focusing on larger momentum transfer and very short-lived nuclei, which are produced with low intensity only.

### 1.2.3. Knockout reactions

Break-up reactions induced by high-energy beams of exotic nuclei allow the exploration of *ground-state configurations* and of excited states. Due to limitations in beam intensity for heavier nuclei, this method has been restricted mainly to light *halo nuclei* so far. Knockout reactions have been used in particular to map the halo nucleon wave function in momentum space, from which their *spatial distribution* is derived via Fourier transformation [Sme99]. By  $\gamma$ -coincidence measurements, different single-particle configurations (including core-excited states) can be identified and corresponding *spectroscopic factors* may be obtained [Aum00]. The coincident measurements of neutrons allow the method to be utilized even if unbound states are involved. As an example, we mention the one-neutron knockout from the two-neutron halo nucleus  $^{11}\text{Li}$  populating states in the unbound nucleus  $^{10}\text{Li}$ , from which the occupancy of the  $(s_{1/2})^2$  and  $(p_{1/2})^2$  configurations of the two halo neutrons in the  $^{11}\text{Li}$  ground state were deduced [Sim99].

At the new facility heavy neutron-rich nuclei, produced by in-flight fission can be studied. With high detection efficiency, secondary beam intensities in the order of ten ions/s are sufficient to extract detailed spectroscopic information, thus making nuclear structure studies possible even very far from stability. Key instruments will be efficient high-resolution  $\gamma$ -ray spectrometers, like the proposed cooled CsI array or AGATA in cases where the ultimate energy resolution is essential. In order to determine the angular momentum  $l$  of the knocked out nucleon, the momentum of the recoil fragment has to be measured with high precision. For medium-mass and heavy nuclei, the required relative momentum resolution is about  $10^{-4}$ , which will be provided by the magnetic spectrometer behind the dipole magnet. Another promising field is the study of *resonant states in the continuum* [Mei02] or even *nuclei beyond the drip lines*, see [Mei03] for a recent study of the unbound  $^5\text{H}$  nucleus.

### 1.2.4. Quasi-free scattering

Knockout reactions using light targets, e.g., Be or C, have proven in the past to be very useful in gaining information on the wave function of the valence nucleons (see 1.2.3.). However, the strong absorption concentrates the reaction probability to the surface. Similar arguments hold for transfer reactions and Coulomb break-up reactions. Nucleon knockout reactions using protons, on the other side, allow one to determine the *spectral functions* of protons and neutrons in a wide range from the weakly bound valence nucleons to the deeply bound core states. Thus, in neutron rich nuclei one gains access to the hitherto unknown region of the strongly bound protons and simultaneously to the valence neutrons. Beside the *single-particle shell-structure*, *nucleon-nucleon correlations* may be investigated as well as *cluster* knockout reactions. For stable nuclei and in normal kinematics, (p,pN) reactions have been used in the past as spectroscopic tool [Kre95].

We intend to develop and apply the technique of quasi-free scattering using radioactive beams in inverse kinematics. At energies around 700 MeV/nucleon (which is high enough to ensure that the conditions for quasi-free scattering are met), both outgoing nucleons have energies in the range where the nucleon-nucleon cross section is at minimum, thus maximizing the transparency of the nucleus and minimizing final state interaction. Measurements such as (p,2p), (p,pn), (p,pd) etc. will become possible in a kinematically complete geometry, allowing a background-free measurement and also for a better control of final state interactions. To detect the proton recoils and other charged particles, we foresee two shells of Si microstrip detectors that surround the liquid hydrogen target integrated into a  $4\pi$  gamma detector (CsI array). For (p,pn) reactions, part of the LAND neutron detector can be placed at angles around 45 degrees to detect the knocked-out neutrons with energies of few hundred MeV. The heavy fragment recoils are momentum analyzed utilizing the high-resolution spectrometer. Thus, the experiment determines the complete kinematics of quasi-free knockout reactions including those to continuum states (by measuring the invariant mass of the decaying system). Even reactions populating states *beyond the dripline* such as, e.g.,  $^{14}\text{Be}(p,p')^{13}\text{Li}$ ,  $^{14}\text{Be}(p,p'\alpha)^{10}\text{He}$ ,  $^{11}\text{Li}(p,p'\alpha)^7\text{H}$ , or  $^8\text{He}(p,p'\alpha)^4\text{n}$ , can be studied.

A thick liquid hydrogen target (200 mg/cm<sup>2</sup>, ~3 cm thickness) will be used. The tracking of both protons and the beam will allow reconstruction of the interaction point with an accuracy much better than 3 mm, corresponding to an effective target thickness of less than 20 mg/cm<sup>2</sup>. Thus, the relative momentum resolution of  $10^{-4}$  for the fragment can be preserved. Experiments can be performed with intensities of 1000 ions/s corresponding to a luminosity of  $10^{26}$  cm<sup>-2</sup>s<sup>-1</sup>.

### 1.2.5. Electromagnetic excitation

Electromagnetic processes in heavy-ion interactions at energies far above the Coulomb barrier give access to a wealth of nuclear structure information on exotic nuclei. At energies of the order of 1 GeV/nucleon, collective nuclear states at low and at high excitation energies are excited in peripheral heavy-ion collisions with large cross sections. Due to Lorentz contraction, the mutual electromagnetic field contains high frequencies up to several tens of MeV/h. *Surface vibrations* and particular *giant resonances* can be studied even with moderate beam intensities. The large cross sections allow experiments with minimum beam intensities of 1 to 1000 ions/s, provided efficient devices for  $\gamma$ -ray and particle detection are implemented.

Electromagnetic excitation of the *giant dipole resonance* induced by high-energy beams on targets of high nuclear charge was pioneered at GSI in exploring the multi-phonon states of the dipole resonance [Aum98]. This method was recently extended to secondary beams of exotic nuclei [Leis01]. It was shown that, e.g., for neutron-rich oxygen isotopes, *low-lying strength* appears and that the usual pattern of the dipole resonance strength distribution dissolves [Leis01]. With the proposed new facility, the measurement of the dipole strength of neutron-rich nuclei relevant for the *astrophysical r-process* will be feasible. In the region of the  $N=82$  closed shell, for instance, the giant dipole strength can be deduced even beyond  $^{132}\text{Sn}$ . For these heavier neutron-rich nuclei, the appearance of a new collective mode is predicted, the collective oscillation of valence neutrons (neutron skin) against the core, the so called *soft dipole mode*. The higher beam intensities also allow the study of giant quadrupole strength. Compared to dipole excitations, the required beam intensities are an order of magnitude larger. Giant resonance studies, in particular monopole and quadrupole excitations, will also be investigated at the NESR using the internal target and at the e-A collider (see the LoI's by the EXL and ELISE collaborations).

Besides resonant excitations, direct non-resonant transitions to the continuum occur for weakly bound nuclei. This 'threshold strength' is characteristic for the *single-particle structure*, being extremely sensitive to the spatial distribution of the valence nucleons. Similar to knockout, the  $l$ -value of the removed nucleon and spectroscopic factors can be deduced [Dat03]. For a halo-like structure, cross sections become very large, and spectroscopic information can be obtained with beam intensities down to 0.1 ions/s.

The continuum structure of drip line nuclei was studied so far only for very light nuclei. From a kinematically complete measurement of the decay not only the excitation spectrum, but also correlations can be studied as, e.g., in the three-body decay of Borromean halo nuclei like  $^{11}\text{Li}$  or  $^6\text{He}$  [Aum99,Ers01]. The experimental technique discussed here also allows the extraction of  $(p,\gamma)$  and  $(n,\gamma)$  reaction rates, which essentially determine the *astrophysical r-, and rp-reaction paths*. While the direct measurement of these rates is very difficult, the  $(\gamma,p)$  and  $(\gamma,n)$  reaction can be measured by electromagnetic excitation using high-energy secondary beams [Sch03] (see subsection 1.2.10).

### 1.2.6. Charge-exchange reactions

The  $(p,n)$  charge-exchange reaction can be used to excite *Gamow-Teller (GT)* and *spin-dipole* resonances by utilizing a liquid hydrogen target and measuring the slow neutrons with plastic scintillators surrounding the target. Studies of the GT strength are beside their importance in nuclear structure of particular astrophysical interest. Electron-capture reactions leading to *stellar collapse and supernova formation* are mediated by GT transitions. Basic understanding of all these processes requires reliable knowledge of the GT strength distribution in a large excitation energy range as well as in nuclei far off stability. Cross sections of the spin-dipole giant resonance excited in  $(p,n)$  reactions are rather directly related to the *neutron skin* thickness. Corresponding measurements were performed so far only for stable isotopes [Kra99]. With exotic nuclear beams, such measurements require secondary beam intensities of the order of 1000 ions/s, and thus a systematic study of neutron skins will be feasible by a method alternative to that consisting of a combination of proton and electron scattering data.

### 1.2.7. Fission

Since fission corresponds to a typical large-scale motion process, it has been recognised as one of the most promising tools for deducing information on *nuclear viscosity*, and on *shell effects* and *collective*

*excitations at extreme deformation*. This is not only important from the fundamental point of view but is of the prime interest in many challenging fields in nuclear physics, like e.g. *super-heavy element synthesis* or nuclide production in secondary-beam facilities. However, many questions still remain open, mainly due to the fact that experiments were restricted up to very recently to spontaneously fissioning isotopes and primordial or long-lived target nuclei. First-generation experiments performed at GSI have proven that the use of secondary beams indeed opens new prospects for studies of nuclear fission [Sch00]. More than 100 short-lived neutron-deficient nuclei will become available for such investigations. From the simultaneous measurement of proton and neutron number of both fission fragments in combination with their velocities, the fission dynamics may be studied in great details (e.g. influences of neutron and proton shells and of pairing correlation, temperature and deformation dependence of nuclear viscosity). The full isotopic distribution of the fission fragments is a sensitive signature of the excitation energy at which fission occurs in the statistical deexcitation cascade. The knowledge of the emitted neutrons and gamma radiation accompanying the fission process allows determining the excitation energies of the final products.

### 1.2.8. Spallation reactions

Spallation reactions are important in various fields of research such as *astrophysics*, *neutron sources* and *production of radioactive beams*. To get a quantitative understanding of the spallation mechanism and to improve its modeling, which is needed for accurate simulations of, e.g., sub-critical reactors coupled with high-intensity proton beams designed as *radioactive waste burners*, exclusive measurements of the reaction channels are mandatory. First experiments in this direction were performed [Duc03] at GSI at the ALADIN/LAND facility with high-energy (1 GeV/nucleon) Fe beams impinging on a liquid hydrogen target. Such studies are most interesting to be extended to heavier systems, which is prohibited at present, however, due to experimental limitations. We intend to measure spallation with two heavy beams,  $^{208}\text{Pb}$  and  $^{238}\text{U}$ . The first one constitutes the main component of the spallation target in accelerator driven systems, while the second allows studying the role of fission in spallation reactions. The R<sup>3</sup>B facility provides the ideal setup for such studies making use of the large-acceptance dipole magnet with its large bending power. The goal will be to identify all the products in mass and nuclear charge (isotopic distributions) of the reactions and measure their velocities so that a complete reconstruction of the excited system at the end of the first stage of the reaction could be achieved. This would allow, for the first time for heavy projectiles, for a detailed study of the competition between the different de-excitation mechanisms (evaporation, fission, emission of intermediate-mass fragments, see also the sections on fission, projectile fragmentation).

### 1.2.9. Projectile fragmentation and multifragmentation

Heavy-ion collisions offer the possibility to probe nuclear matter under different conditions of densities and temperatures. In multifragmentation, nuclear matter at low densities and, more generally, modes of disintegration of dynamically unstable systems are probed. In particular, the expected link with the *nuclear liquid-gas phase transition* provides a continuing motivation for studying multifragmentation. In these reactions, systems of small and intermediate-mass nuclei surrounded by a nucleon gas may be produced, with properties close to what is expected in stellar processes as, e.g., supernova II explosions [Bot04]. Also properties of the high-density zones of the collision may be studied in the fragmentation of excited projectile spectators. The velocities of projectile residues are predicted to be sensitive to the non-local features of the nuclear mean field [Ric03].

Isotopic effects in multifragmentation, originating from the two-fluid nature of nuclear matter [Mue95], reflect the strength of the *symmetry term* in the *equation of state* whose density dependence is of importance for astrophysical applications. Experiments using the existing GSI facilities [Ala03] have shown that secondary beams of exotic nuclei are useful and necessary for obtaining systems with a sufficiently broad range of isotopic composition. With the new facility, this can be further extended, in particular to neutron-rich asymmetric matter for which the effects of the symmetry term are most strongly pronounced.

Projectile fragmentation of secondary beams in conjunction with *γ-ray spectroscopy* is a powerful method to explore *excited states in exotic nuclei*. This method is also addressed in the LEB LoI. The R<sup>3</sup>B

setup is particularly well suited for cases at the very limits of the production rates, i.e., for the most exotic nuclei. Here, the better transmission using high-energy beams and the high efficiency of the CsI  $\gamma$ -array is advantageous.

### 1.2.10. Astrophysics

Reactions, which are of particular interest for astrophysics, were already mentioned in the previous subsections. These are Gamow-Teller transitions measured by charge-exchange reactions, spallation reactions, and Coulomb dissociation. The nuclei that will be accessible with the NUSTAR facility will allow exploring the reactions inverse to those relevant for the astrophysical rp- and r-processes by utilizing the electromagnetic excitation process at high beam energy. The cross sections for the direct capture reactions in the stellar environment are very small due to the stellar temperature ( $\sim 20$  keV) and the Coulomb barrier, while the cross sections for the inverse process, Coulomb dissociation, are much larger. Of special interest are the  $(\gamma, p)$  and  $(\gamma, n)$  cross section at very low fragment-nucleon relative energy. The proton tracking through the magnetic field of the large acceptance dipole will result in a momentum resolution of  $10^{-3}$ . For the neutrons, a similar resolution is achievable by making use of a long time-of-flight path of  $\sim 35$  m (ToF resolution  $< 100$  ps), resulting in an invariant-mass resolution of better than 20 keV (at 100 keV relative energy), thus making cross-section measurement feasible at energies relevant for astrophysics, down to about 10 keV. Here, the lead target thickness is limited to about  $100$  mg/cm<sup>2</sup> due to multiple scattering and energy loss. Still, with beam intensities of  $\sim 10^4$  ions/s differential cross sections of  $100$   $\mu\text{b}/(10$  keV bin) can be measured within a few days.

## 2. Detector subsystems

### 2.1. Superconducting large-acceptance dipole

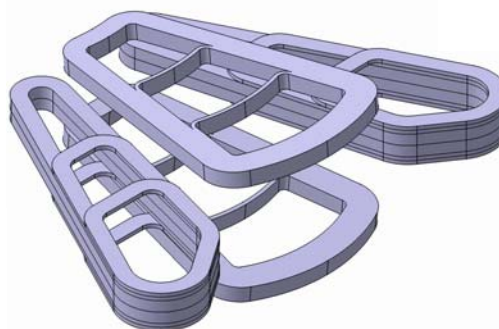


Figure 2: Layout of the four superconducting coils of the R<sup>3</sup>B dipole. The side coils are optimized to reduce the fringe fields. The field integral amounts to about 5 Tm.

For the variety of experiments to be performed, a zero-degree superconducting dipole magnet was designed for the R<sup>3</sup>B project. The main parameters of the spectrometer are: (i) A large vertical gap providing an angular acceptance of  $\pm 80$  mrad for neutrons; (ii) A maximum bending angle of  $40^\circ$ , ensuring an acceptance close to 100% even for experiments with very different magnetic rigidities of the beam and the fragments; (iii) A high field integral of about 5 Tm, which allows a bending angle of  $18^\circ$  for a 15 Tm beam (e.g. 1 GeV/nucleon <sup>132</sup>Sn or 500 MeV/nucleon <sup>8</sup>He) or  $14^\circ$  for 20 Tm beams, the maximum rigidity provided by the Super-FRS. A momentum resolution of up to  $10^{-3}$  can be achieved by tracking the particles with high resolution. The design includes four super-conducting coils, shown in Figure 2, which are tilted to match the required acceptance angle for the particles of interest. The side coils are optimized to reduce the fringe field, and guarantee a low magnetic field in the target region, where detectors have to be placed. A technical design report is available ( <http://www-land.gsi.de/r3b/docu/TDR-R3B-dipole.pdf> ). An application for funding the construction of the dipole has been submitted to the European Commission.

### 2.2 High-resolution spectrometer

A high-resolution magnetic spectrometer is foreseen for experiments demanding a precise momentum analysis after the target. This is particularly important for heavy beams ( $A > 100$ ), e.g., for quasi-free scattering and knockout reaction, where the momentum of the recoiling ( $A-1$ ) fragments has to be analyzed in order to deduce the angular momentum of the knocked out particle from their momentum

distributions. A resolution of 20 to 50 MeV/c is required, corresponding to a relative momentum width  $\Delta p/p \sim 10^{-4}$  for heavy beams. Other experiments with similar demands were discussed in the previous sections. For that purpose, the large-acceptance dipole will be operated in reversed mode deflecting the fragments into the magnetic spectrometer (see Figure 1). The possibility of deflecting the beam in both directions, allows keeping a permanent setup for both experiments ('large-acceptance' and 'high-resolution' mode). Possible spectrometer solutions will be investigated in the near future. As a starting point, the use of dipoles identical to the Super-FRS design is considered, thus reducing the costs. Since the acceptance of the Super-FRS ( $\pm 2.5\%$ ) is large compared to the momentum transfer in the reaction, the emittance does not increase much (if only one reaction channel is considered), and it is sufficient to have the same acceptance before and after the target. In conjunction with fragment tracking, a resolution of  $\Delta p/p \sim 10^{-4}$  seems to be achievable for momentum determination of the incident beams as well as for the outgoing fragments. Determining the momentum via tracking of the beam particles has the advantage compared to a dispersion matching scheme that the focus at the reaction target has not to be dispersive, thus avoiding a large beam spot at the target. Detailed calculations concerning acceptance and achievable resolution are in progress. The deflection of the fragments by the large-acceptance magnet into the spectrometer allows zero-degree operation (e.g. for knockout reactions or quasi-free scattering), but also enables measurements at larger angles by adjusting the magnetic field of the sweeper magnet.

### 2.3 Tracking detectors and velocity measurements

Various tracking detector systems with different demands are required. The incoming beam will be tracked (starting from the dispersive focus at the Super-FRS) in order to determine beam momentum, angle and position incident on the target, and, similarly, for the spectrometer after the target. In order to achieve the optimum momentum resolution, it is mandatory that the angular scattering induced by these tracking detectors being as small as possible. Silicon micro-strip, diamond strip, as well as position sensitive channel-plate detectors are considered. First prototype tests have already been started. For the large-acceptance mode, large-area detectors are placed behind the R<sup>3</sup>B dipole magnet. For detection of light charged particles drift chambers with a size of about  $1.2 \times 0.6 \text{ m}^2$  including dedicated front-end electronics are presently being considered.

The velocity of the incoming beam as well as of the fragments has to be determined with a resolution of  $10^{-3}$  in order to achieve unique isotope identification after the target also for heavy beams. Such a resolution is provided by a Cherenkov detector. The thickness of the Cherenkov radiator, however, represents a substantial target in the beam and further developments are needed in order to improve the situation significantly. For the large-acceptance mode, the flight path of the fragments amounts to about 10 m only, thus a time resolution for the ToF measurement of better than 40 ps is required. A time-of-flight wall consisting of fast scintillating material and ultra-fast phototubes is considered. First tests to explore the achievable time-resolution involving relatively large detector arrays ( $\sim 1 \text{ m}^2$ ) have been started. The very successful developments in resistive-plate chambers (RPC) might also provide an alternative solution.

### 2.4 Gamma detection

#### *Total $\gamma$ -absorption spectrometer*

A  $4\pi$   $\gamma$ -calorimeter array surrounding the target with high efficiency and angular resolution is foreseen. At beam energies of typically 700 MeV/nucleon, the gamma energies are Lorentz boosted by a factor 2 to 3 in the forward directions at angles between 10 and 30 degree, where most of the intensity is located. Consequently, the photon detector should have a high absorption probability for photons with energies up to 10 MeV. Besides the  $\gamma$ -sum energy the detector has to provide  $\gamma$ -multiplicity and individual  $\gamma$ -energies for spectroscopy purposes. To obtain a proper  $\gamma$ -sum energy the strong angle dependent Doppler shift of individual  $\gamma$ -rays needs to be corrected for. Thus a granularity in the order of 1000 is required to maintain the intrinsic resolution of  $\approx 2\%$  obtainable with novel cost effective scintillation detectors. An "egg"-shaped array with asymmetric target position and increasing detector thickness at forward angles is anticipated. A sum energy efficiency of  $\epsilon_{\text{sum}} > 80\%$ , a sum-energy resolution of  $\sigma(E_{\text{sum}})/\langle E_{\text{sum}} \rangle$  below 10% and a multiplicity resolution of  $\sigma(N_{\gamma})/\langle N_{\gamma} \rangle$  better than 10% is

envisaged. The corresponding photo-peak efficiency is  $\varepsilon > 50\%$  (at  $E_{\gamma}^{lab}=10$  MeV) with a  $\gamma$ -energy resolution of 2%.

Design studies concerning possible and most economic solutions just started. One idea is to build an array consisting of cooled scintillators (e.g. undoped CsI or NaI). As alternative new inorganic scintillation materials like LaBr<sub>3</sub> need to be investigated. The light read-out of the scintillators will be performed by PIN diodes. The array will also be used for detecting and measuring the total energy of protons from quasi-free scattering in conjunction with a  $2\pi$  array of light particle detectors.

#### *High resolution $\gamma$ -spectrometer*

For high-resolution  $\gamma$ -spectrometry a forward wall of AGATA Ge tracking detectors (see LEB LOI) is foreseen. Employing half of the AGATA detectors in a compact arrangement covering the angular range from  $9^{\circ}$  to  $45^{\circ}$  at a target distance of 50 cm will result in a photo-peak efficiency of  $\varepsilon \approx 12\%$  (for  $E_{\gamma}=1.3$  MeV in the projectile rest frame). The corresponding energy resolution will be about 0.5% for a nucleus with a kinetic energy of 700 MeV/nucleon.

### **2.5 Proton recoil detector**

In the quasi-free scattering (knockout) reaction, the knocked-out nucleon and the target (proton) recoil are scattered typically in a range between  $20^{\circ}$  and  $70^{\circ}$ , both having energies between 200 and 500 MeV (assuming beam energies around 700 MeV/nucleon). According to kinematical calculations, the detection setup for the recoil particles should consist of two layers of double sided Si micro-strip detectors, organized as barrels to cover the forward direction. The advantage of using such detectors is that very precise position and good energy loss information is provided. The first layer of the detector will be placed as close as possible to the target to improve the precision of vertex determination while minimizing the size (and the cost) of the first shell. The distance between the first and the second shell will be as small as possible, while compensating the lack of distance between the shells (for the tracking) by the high position resolution of the detectors (50  $\mu\text{m}$  or better). 300  $\mu\text{m}$  thick Si detectors for the second layer and 100  $\mu\text{m}$  (or less to reduce multiple scattering) for the first layer, are considered. Chips with high dynamic range will allow also the detection of  $\alpha$ -particles in case of using liquid helium target. The required angular resolution of 2 to 3 mrad is achievable with this type of detectors. The total energy of the recoils should be measured by the surrounding  $4\pi$  sphere of scintillator (CsI, see 2.4), serving also to detect  $\gamma$ -rays. The detector will also be used as multiplicity detector (target hodoscope) for experiments dedicated to semi-peripheral collisions to obtain information on impact parameter and reaction plane.

Some of the reaction studies listed in Table 1 (i.e. elastic and inelastic scattering) require in special cases high resolution measurement of target-like reaction products at very low momentum transfer which is not possible with the standard target-detector setup. Such investigations are most favourably performed at the internal target of the NESR (see EXL LOI) for all cases where the lifetime of the exotic beam is sufficiently long ( $>500$  ms) to allow for beam preparation in the CR/NESR rings. In contrast, for the case of very short-lived nuclei, the concept of an active target, where target and detector medium are identical, is considered. This detector concept has already been successfully applied for light exotic beams in experiments at GSI [Neu02] and GANIL [Dem03] and will be further developed for applications with heavy exotic beams by the ACTAR collaboration [ACTAR proposal to EURONS].

### **2.6 Low-energy neutron detector**

In case of (p,n) charge-exchange reactions, the angle and energy of the low-energy neutron has to be detected from which the angular momentum transfer and the excitation energy is determined. In order to achieve the envisaged excitation-energy resolution of 1 MeV, an energy resolution of 10% and angular resolution of  $1^{\circ}$  for the neutron is required. This can be achieved by placing 4 cm thick plastic scintillators (30% efficiency) at a distance of about 1 m from the target (ToF resolution  $\sim 1$  ns, flight time for a 5 MeV neutron is about 30 ns). Prototype tests are going on. The optimum geometry is presently being studied in Monte Carlo simulations.

### 2.7 High-resolution neutron time-of-flight spectrometer

The large-area neutron detector LAND is presently used to detect high-energy neutrons and determine their momenta via ToF and position measurement (obtained from a time difference measurement). The iron-converter/scintillator sandwich structure results in a rather high efficiency of more than 90% for neutron energies above 400 MeV. The obtained invariant-mass resolution is determined mainly by the time resolution of LAND. A better time resolution in the order of 100 ps is envisaged by using fast scintillating materials and ultra-fast phototubes for the NewLAND detector. Together with a long flight path of 35 m, high-resolution measurements will become possible. This is particularly important for, e.g., the measurement of  $(\gamma, n)$  reactions relevant for astrophysics. Cross sections could be measured down to 10 keV fragment-neutron relative kinetic energy.

### 2.8 Multi-track ion detector for spallation and fission measurements

In order to detect multi-particle final states of spallation reactions or the two fragments in fission experiments, a multi-track detector has to be installed downstream of the R<sup>3</sup>B dipole magnet. Two main goals have to be reached with this multi-track detector: i) The spectrometry of reaction fragments at the  $10^{-3}$  level in momentum resolution in the laboratory frame; ii) The nuclear charge identification of these fragments from  $Z = 1$  to  $Z = 92$ . Furthermore, this detector has to provide a detection efficiency very close to 100 % even for light fragments ( $Z = 1$  or 2) in order to minimize efficiency corrections to measure cross-sections in a many-fold (multi-particle) final state phase space.

For light reaction products, such a detector will allow for the reconstruction of the kinematics at the reaction point in angle and momentum and thus for the kinematical reconstruction of the variables in the center of mass frame. For heavy fragments, fission products or projectile evaporation residues, the magnetic rigidity of the fragments with a resolution in mass of  $A/\Delta A \sim 300$  (*FWHM*) has to be determined by combining the information with the measurements from the detectors upstream from the dipole. To achieve this, a spatial resolution of roughly 100  $\mu\text{m}$  has to be aimed at in the detector design.

This detector will have to assure a multiple sampling measurement of trajectories. There are two reasons for this: i) To perform  $Z$  identification with  $\Delta E$  measurements, the sampling of the primary energy loss signal has to be large enough (to be specified quantitatively, depending on the detector and its active material); ii) To avoid the huge combinatorial of points, which has to be considered when working with partial information from planes of wires from MWPC's.

A gaseous detector such as a time projection chamber (TPC) is considered with vertical drift lines for the primary signals in order to assure the highest position resolution in the horizontal plane (the magnet dispersive plane) by center of gravity determination using the charges collected on the pads, and multi-hit readout with flash-ADCs in order to distinguish two trajectories on the top of each other in the detector. Further developments of the ALADIN MUSIC detector concept are also considered.

## 3. Trigger and data-acquisition system

Experiments with secondary beams at the Super-FRS require a determination of the projectile and fragment masses before and after the secondary reaction target, respectively. This involves measuring time of flight (ToF) and magnetic rigidity ( $B\rho$ ). Since ( $B\rho$ ) of an ion can only be determined at a dispersive focal plane of the Super-FRS, the corresponding position measurements are performed at rather large distances from each other. Likewise, the detectors for detecting neutrons, charged particles, or decay radiation are located far from each other. The R<sup>3</sup>B data acquisition concept, therefore, foresees distributed subsystems that acquire data (position, time, energy loss, decay radiation etc.) in self-triggered mode synchronized by time stamps; sub-events are sent to the event builder via fast optical links. These subsystems will be designed along the same lines as the present RISING distributed readout. It is also very likely that developments underway at other experiments (e.g. within the EU project I3HP with their more ambitious requirements) will provide solutions for front-end preprocessors, high-speed data links, or time-stamp distribution that can be adapted to the needs of R<sup>3</sup>B, thereby making use of synergetic effects.

Following current trends, we foresee largely digital electronics based on ultra-fast sampling of the direct or preamplifier signals, followed by digital signal processing rather than analog pulse shaping or time

pick-off. These concepts have been successfully applied at the present FRS for measuring atomic masses in the ESR via the ToF method, and are indispensable for the readout of future  $\gamma$ -ray tracking detectors like AGATA. Whereas at present such approaches rely largely on expensive commercial modules with small numbers of channels, efforts will concentrate on designing custom-built inexpensive modules that allow digitizing economically the few thousand channels foreseen in R<sup>3</sup>B. A common data-acquisition system for the NUSTAR experiments is aimed for.

## 4. Physics performance

To a large extent, the proposed setup bases on further developments of the existing LAND reaction setup at GSI. The concept and design of the experimental setup addressed in this LoI, and the corresponding estimates on resolution and performance are based on the expertise that has been gained from experiments and developments at the present facility. The existing setup will be extremely instrumental in designing and testing detector prototypes. Several of the developments discussed above will be implemented already for experiments using radioactive beams in Cave C. Ion-optical calculations for the design of the magnetic spectrometer are on the way, which are the basis for simulations exploring the limits in achievable momentum resolution implying tracking through the spectrometer. Such studies will also define the demands on detector design concerning thickness and resolution. The designs of the proton-recoil detector as well as the total-absorption gamma spectrometer will be based on GEANT simulations as well as on tests of prototype detectors and electronics. The final conceptual and technical design together with the simulation results will be presented in technical design reports to be worked out by the collaboration.

## 5. Implementation

### 5.1 Experimental area and radiation environment

The R<sup>3</sup>B experiment will be located at the focal plane of the high-energy branch of the Super-FRS. An experimental hall of about 50 m length and 20 m wide is required (depending on the final design of the magnetic spectrometer) with standard technical infrastructure including crane and cooling system for the super-conducting magnets. Access has to be provided to bring in large and heavy equipment. The height of the beam line should be at least 2.0 meter. Typical beam intensities used for R<sup>3</sup>B experiments will range between few ions/s up to  $10^7$  ions/s. All beams up to uranium have to be considered. The cave should be accessible independent of operation of other Super-FRS beam lines, e.g., the ring branch and the low-energy branch.

### 5.2 Cost estimates

The costs for the planned R<sup>3</sup>B setup are dominated by the investments needed for the large-acceptance dipole (5.7 MEuro) and the high-resolution magnetic spectrometer, see Table 2. Only a preliminary and rough cost estimate can be given since the designs for many detectors and the high-resolution spectrometer are not finalized. For the magnetic spectrometer, the costs for two Super-FRS dipole stages were assumed ( $\sim 8$  MEuro). An application was submitted to the European Commission for funding of the construction of the large-acceptance dipole within the 6<sup>th</sup> framework programme. If the proposal will be accepted, construction costs of 5.0 MEuro will be funded by the EU.

Table 2. Preliminary cost estimate

Task	Cost estimate (MEuro)
Quadrupole triplet in front of the target	1.0
Super-conducting large-acceptance dipole magnet	5.7
High-resolution magnetic spectrometer	8.0
Total-absorption gamma spectrometer	2.0
High-resolution time-of-flight neutron detector	2.2
Heavy-ion and charge particle detectors incl. readout electronics	0.8
Total	19.7

### 5.3 Organisation and responsibilities

The research teams forming the R<sup>3</sup>B collaboration have a large experience with regard to the scientific and technological aspects addressed in this LoI and will participate according to their expertise and physics interest. Table 3 gives an overview on the tasks and a tentative list of institutes involved in the working groups in charge for the individual developments. Names of responsible persons are given for each institute; those having a coordinating role for the specific sub-task are indicated with *italics*. A coordination board (CB) will be formed out of representatives of the participating groups taking over major duties in developments. The role of this board will be to ensure overall monitoring of the quality and progress of the developments. The CB will consist of about 10 members including the spokespersons of the collaboration.

Table 3. List of tasks and tentatively assigned working groups and responsibilities

Task	Group
Spokespersons	T. Aumann, B. Jonson
Large-acceptance dipole	CEA Saclay ( <i>J.E. Ducret</i> , <i>B. Gastineau</i> ), GSI ( <i>T. Aumann</i> )
High-resolution spectrometer	Argonne ( <i>J. Nolen</i> ), Giessen ( <i>M. Winkler</i> ), GSI ( <i>T. Aumann</i> ), MSU ( <i>B. Sherrill</i> ), UK ( <i>R. Lemmon</i> )
Tracking detectors	CEA Saclay ( <i>A. Boudard</i> , <i>J.E. Ducret</i> ), FZ Rossendorf ( <i>A. Wagner</i> ), GSI ( <i>T. Aumann</i> , <i>A. Kelic</i> , <i>K. Sümmerer</i> ), St. Petersburg ( <i>A. Khanzadeev</i> ), TU München ( <i>R. Gernhäuser</i> , <i>R. Krücken</i> )
ToF measurements	Santiago ( <i>J. Benlliure</i> ), CEA Saclay ( <i>E. Pollacco</i> ), GSI ( <i>K. Sümmerer</i> ) Krakow ( <i>R. Kulesa</i> )
Total-absorption gamma spectrometer	GSI ( <i>J. Gerl</i> ), MPI Heidelberg ( <i>H. Scheit</i> ), Uni Köln ( <i>P. Reiter</i> ), TU München ( <i>R. Krücken</i> ), UK ( <i>K. Spohr</i> ), Valencia ( <i>B. Rubio</i> ), Kolkata ( <i>U. Datta Pramanik</i> )
Proton recoil detector	CEA Saclay ( <i>E. Pollacco</i> ), Chalmers ( <i>B. Jonson</i> ), Uni Mainz ( <i>O. Kisselev</i> ), GSI ( <i>P. Egelhof</i> , <i>H. Emling</i> ), Kurchatov ( <i>L. Chulkov</i> ), GANIL ( <i>W. Mittig</i> ), TU Darmstadt ( <i>T. Nilsson</i> ), UK ( <i>R. Lemmon</i> )
Low-energy neutron detector	Debrecen ( <i>A. Krasznahorkay</i> ), GSI ( <i>H. Emling</i> )
Neutron ToF spectrometer	GSI ( <i>H. Emling</i> ), Krakow ( <i>R. Kulesa</i> ), Santiago ( <i>J. Benlliure</i> )
Multi-track ion detector	CEA Saclay ( <i>J.E. Ducret</i> ), GSI ( <i>K.-H. Schmitt</i> ), IPN Orsay ( <i>Ch.O. Bacri</i> )
DAQ	GSI ( <i>H. Simon</i> ), Krakow ( <i>R. Kulesa</i> ), TU München ( <i>M. Böhmer</i> ), UK ( <i>I. Lazarus</i> )
Simulations	Aarhus ( <i>K. Riisager</i> ), Chalmers ( <i>B. Jonson</i> ), Orsay ( <i>Ch.O. Bacri</i> ), Madrid ( <i>M. Borge</i> ), Santiago ( <i>D. Cortina</i> ), Valencia ( <i>J.L. Tain</i> ), UK ( <i>M. Labiche</i> )
(UK collaboration: Uni Keele, Uni Surrey, Uni Liverpool, Uni Manchester, Uni Birmingham, CCLRC Daresbury, Uni York, Uni Paisley)	

### Synergies with other LoI's

Several detector developments and in particular the readout electronic and data acquisition systems are to a large extent similar to those discussed, e.g., for the experiments using internal targets in the storage ring (see EXL LoI) and the electron scattering experiment at the e-A collider (see ELISe LoI). Of course, such synergetic effects have to be exploited. A close collaboration among the participants of R<sup>3</sup>B, EXL and ELISe is therefore desired.

### 5.4 Time schedule

According to the time plan for the construction of the Super-FRS, the high-energy beam line will be the first operational, starting commissioning in 2011. Consequently, the experimental setup will be moved to the new experimental area in 2010, and first experiments may be expected to start in 2011. Most of the detector developments are intended to be ready already for first experiments to be performed in Cave C using the current FRS. The high-resolution magnetic spectrometer will be built and installed in the new hall in parallel with the construction of the Super-FRS.

Table 4. Time schedule for implementation of the R<sup>3</sup>B experiment

	2003	2004	2005	2006	2007	2008	2009	2010	2011
Large-acceptance dipole									
High-resolution spectrometer									
Tracking detectors									
proton arm									
large-area ion and ToF det.									
Super-FRS and spectrometer									
Total-absorption $\gamma$ -detector									
Proton-recoil detector									
Low-energy neutron detector									
Neutron ToF detector									
Move setup into new Cave									
Simulations, R&D, design									
Installation, tests									
	Prototyping, construction								
	Commissioning, experiments								

### 5.6 Beam time considerations

Typical experiments to be performed at R<sup>3</sup>B need two to three weeks of beam time. A total requirement of 3 months/year beam on target is estimated. The experiment requires DC or DC like beams. In most cases, secondary beams will be used, which will be produced and separated with the Super-FRS. Most experiments will ask for the maximum reachable intensity with energies up to 1500 MeV/nucleon. This means that SIS100 as well as SIS300 (as stretcher ring) will be needed. The use of the Super-FRS implies that no other experiments with radioactive beams, e.g., low-energy branch or ring branch, can be operated in parallel. Parallel operation with other programmes is possible to some extent, which will, however, reduce the duty cycle implying longer runs in consequence.

### References

- [Ala03] K. Kezzar *et al.*, (ALADIN-FRS-LAND collaborations), SIS experiment S254.
- [AlK03] J. Al-Khalili and F. Nunes, *J. Phys. G* 29 (2003) R89.
- [Aum98] T. Aumann, P.F. Bortignon, H. Emling, *Annu. Rev. Nucl. Part. Sci.* 48 (1998) 351.
- [Aum99] T. Aumann *et al.*, *Phys. Rev. C* 59 (1999) 1252.
- [Aum00] T. Aumann *et al.*, *Phys. Rev. Lett.* 84 (2000) 35.
- [Bot04] A.S. Botvina and I.N. Mishustin, *Phys. Lett. B* 584 (2004) 233.
- [Dat03] U. Datta Pramanik *et al.*, *Phys. Lett. B* 551 (2003) 63.
- [Dem03] C.E. Demonchy, PHD-thesis, Univ. of Caen (2003), Ganil T 03 06.
- [Duc03] J.E. Ducret *et al.*, SPALADIN experiment, performed at GSI, proposal S248.
- [Ege02] P. Egelhof *et al.*, *Eur. Phys. J. A* 15 (2002) 27.
- [Ers01] S.N.Ershov, B.V.Danilin and J.S.Vaagen, *Phys. Rev. C* 64 (2001) 064609.
- [Kra99] A. Kraznahorkay *et al.*, *Phys. Rev. Lett.* 82 (1999) 3216.
- [Kre95] G. Krein, Th.A.J. Maris, B.B. Rodrigues, E.A. Veit, *Phys. Rev. C* 51 (1995) 2646.
- [Lei01] A. Leistenschneider *et al.*, *Phys. Rev. Lett.* 86 (2001) 5442.
- [Mei02] M. Meister *et al.*, *Phys. Rev. Lett.* 88 (2002) 102501.
- [Mei03] M. Meister *et al.*, *Phys. Rev. Lett.* 91 (2003) 162504.
- [Mue95] H. Müller and B.D. Serot, *Phys. Rev. C* 52 (1995) 2072.
- [Neu02] S.R. Neumeier, *Nucl. Phys. A* 712 (2002) 247.
- [Ric03] M.V. Ricciardi *et al.*, *Phys. Rev. Lett.* 90 (2003) 212302
- [Sch00] K.-H. Schmidt *et al.*, *Nucl. Phys. A* 665 (2000) 221.
- [Sch03] F. Schümann *et al.*, *Phys. Rev. Lett.* 90 (2003) 232501.
- [Sme99] M.H. Smedberg *et al.*, *Phys. Lett. B* 452 (1999) 1.
- [Sim99] H. Simon *et al.*, *Phys. Rev. Lett.* 83 (1999) 496.
- [Suz95] T. Suzuki *et al.*, *Phys. Rev. Lett.* 75 (1995) 3241.